

Bulges *versus* discs: the evolution of angular momentum in cosmological simulations of galaxy formation

Jesus Zavala^{1*}, Takashi Okamoto², Carlos S. Frenk²

¹*Instituto de Ciencias Nucleares, Universidad Nacional Autónoma de México A.P. 70-543, México 04510 D.F., México*

²*Institute for Computational Cosmology, Department of Physics, Durham University, South Road, Durham, DH1 3LE*

Accepted —. Received —; in original form —

ABSTRACT

We investigate the evolution of angular momentum in simulations of galaxy formation in a cold dark matter universe. We analyse two model galaxies generated in the N-body/hydrodynamic simulations of Okamoto et al. Starting from identical initial conditions, but using different assumptions for the baryonic physics, one of the simulations produced a bulge-dominated galaxy and the other one a disc-dominated galaxy. The main difference is the treatment of star formation and feedback, both of which were designed to be more efficient in the disc-dominated object. We find that the specific angular momentum of the disc-dominated galaxy tracks the evolution of the angular momentum of the dark matter halo very closely: the angular momentum grows as predicted by linear theory until the epoch of maximum expansion and remains constant thereafter. By contrast, the evolution of the angular momentum of the bulge-dominated galaxy resembles that of the central, most bound halo material: it also grows at first according to linear theory, but 90% of it is rapidly lost as pre-galactic fragments, into which gas had cooled efficiently, merge, transferring their orbital angular momentum to the outer halo by tidal effects. The disc-dominated galaxy avoids this fate because the strong feedback reheats the gas which accumulates in an extended hot reservoir and only begins to cool once the merging activity has subsided. Our analysis lends strong support to the classical theory of disc formation whereby tidally torqued gas is accreted into the centre of the halo conserving its angular momentum.

Key words: methods: numerical – galaxies: evolution – galaxies: formation

1 INTRODUCTION

In the standard theory of galaxy formation in the cold dark matter (CDM) cosmogony, disc galaxies form when rotating gas cools inside a dark matter halo and fragments into stars. Analytic and semi-analytic calculations of this process start by assuming that tidal torques at early times impart the same specific angular momentum to the gas and the halo and that the angular momentum of the gas is conserved during the collapse (Fall & Efstathiou 1980; Mo et al. 1998; Cole et al. 2000; Firmani & Avila-Reese 2000). It is unclear whether this assumption holds in gasdynamic simulations of galaxy formation.

The first attempts to simulate the formation of a spiral galaxy from cold dark matter initial conditions generally failed, producing objects with overly centrally concentrated distributions of gas and stars. It became immediately apparent that the root cause of this problem was a net transfer of angular momentum from the baryons to the dark matter halo during the aggregation of the galaxy

through mergers (Navarro & Benz 1991; Navarro & White 1994; Navarro, Frenk, & White 1995). This is known as the “angular momentum problem”. It was suspected from the start that its solution was likely to involve feedback processes that would regulate the supply of gas to the galaxy.

More recent simulations within the CDM framework have produced more promising disc galaxies. Thacker & Couchman (2001) obtained a reasonably realistic disc at $z = 0.5$ (when their simulation stopped) by assuming that gas cooling is strongly suppressed by feedback effects. Steinmetz & Navarro (2002), using different prescriptions for star formation and feedback, found that a broad range of galaxy morphologies could be produced. In related work, Abadi et al. (2003) obtained a disc galaxy with a realistic density profile but not enough angular momentum. Sommer-Larsen, Götz, & Portinari (2003) found that considerably larger energy feedback rates at early times than previously employed were required to ameliorate the angular momentum problem. They achieved this by distinguishing between *early* and *late* star formation modes, assuming a higher star formation efficiency and stronger feedback in the early mode. They were able to generate a variety of morphological types, including discs whose an-

* Present address: Shanghai Astronomical Observatory, Nandan Road 80, Shanghai 200030, China; jzavala@shao.ac.cn

gular momentum, however, was still a factor of two smaller than observed for real disc galaxies.

Governato et al. (2004) produced a disc galaxy without requiring strong feedback and ascribed the angular momentum problem to a lack of numerical resolution. However, subsequently, Governato et al. (2007) were forced to invoke strong feedback in order for their simulated discs to lie closer to the Tully-Fisher relation. While resolution is clearly an important and complicated issue, Okamoto et al. (2003) argued that if the hot and cold gas components are decoupled from each other, then the effects of resolution in the current generation of simulations are reduced. Robertson et al. (2004) adopted a multiphase model for the star-forming interstellar medium (ISM) which stabilises gaseous discs against the Toomre instability, and produced a galaxy with an exponential surface brightness profile but insufficient angular momentum in the inner parts. They concluded that the fragmentation of gaseous discs caused by the Toomre instability is the main cause of the angular momentum loss in simulations that usually assume an isothermal ISM at a temperature of $\sim 10^4$ K.

Okamoto et al. (2005) also adopted a multiphase model for the ISM and assumed a top-heavy initial mass function (IMF) for stars formed in starbursts. The latter assumption was motivated by the semi-analytic model of Baugh et al. (2005) which requires a large relative abundance of massive stars in order to match the number counts of bright submillimeter galaxies. A top-heavy IMF is further supported by the good agreement of this model with the metal abundances measured in the intracluster medium (Nagashima et al. 2005a) and in elliptical galaxies (Nagashima et al. 2005b). By varying the criteria for starbursts in their simulations, Okamoto et al. (2005) were able to produce galaxies with a variety of morphological types, from ellipticals to spirals, starting from exactly the same initial conditions. They showed that disc galaxies can form in halos that have a relatively quiet merger history if the early collapse of baryons is inhibited by strong feedback, in this case generated by the evolution of a stellar population with a top-heavy IMF.

In this paper, we analyse two of the galaxies simulated by Okamoto et al. (2005), one which ended up as a bulge-dominated galaxy and another that formed an extended stellar disc. We trace the time evolution of the angular momentum of the dark matter and the gas, and we distinguish between the evolution of the inner part of the dark halo and the halo as a whole. We show explicitly that mergers transfer angular momentum from the inner parts of the system to the outer halo. This process is one aspect of the redistribution of angular momentum during virialization investigated in N-body simulations by D’Onghia et al. (2006) and D’Onghia & Navarro (2007). Thus, the spin of the *central* part of the final system contains a fossil record of the merger history of the object.

This paper is organised as follows. The simulations are briefly described in Section 2. The method we use to follow the angular momentum of the different components is explained in Section 3 where we also present our results. We conclude in section 4.

2 THE SIMULATIONS

Details of the simulations that we analyse here may be found in Okamoto et al. (2005). The initial conditions were extracted from a cosmological N-body simulation (of a cubical region of side $35.325h^{-1}$ Mpc) and correspond to a dark matter halo of present day virial mass $M_{\text{vir}} \simeq 1.2 \times 10^{12} h^{-1} M_{\odot}$ which has a quiet merging history since $z \sim 1$. The simulations were carried out using

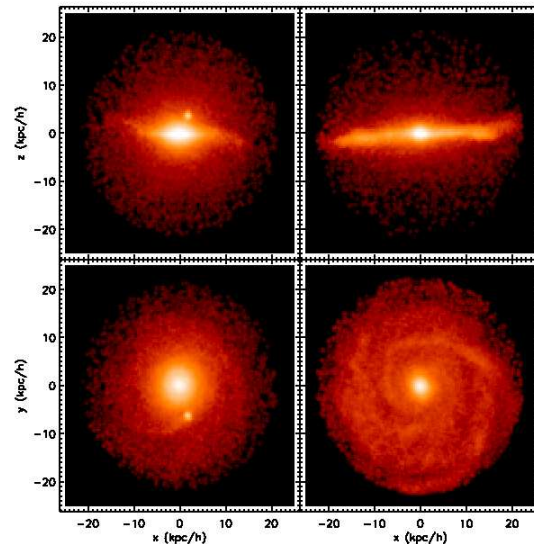


Figure 1. Edge-on (top) and face-on (bottom) views of the baryonic component of the bulge-dominated (left) and disc-dominated (right) galaxies. Stars and gas with $\rho_g \geq 7 \times 10^{-27} \text{ gr cm}^{-3}$ within 10% of the virial radius make up the baryonic component. The brightness indicates the projected mass density.

the N-body/SPH code GADGET-2 (Springel 2005). They include a multiphase description of the star-forming gas and make use of the ‘phase-decoupling’ technique introduced by Okamoto et al. (2003) to suppress the spurious angular momentum transfer from cold disc gas to ambient hot halo gas which would otherwise arise from the very nature of SPH.

One of the two simulations that we analyse is the “no-burst” model which has a standard prescription for star formation, tuned to reproduce the local Kennicutt (1998) relation between star formation rate and gas density. This simulation yielded a galaxy with a large bulge and a small disc, to which we will henceforth refer as the “bulge-dominated” galaxy (left panels in Fig. 1).

The second simulation is the “shock-burst” model in which the star formation efficiency is higher than average in gas that has recently been shock-heated. The stellar populations that form from this gas in a starburst are assumed to have a top-heavy IMF. Thus, in this model there is additional supernova heating available when galaxies merge. The outcome of this simulation was a galaxy with a large disc and a small bulge – the “disc-dominated” galaxy (right panels in Fig. 1). The (kinematically identified) disc in this galaxy contains 48% of the stellar mass and 84% of the B-band light, making this a good candidate for a late-type spiral. However, the surface brightness distribution of the disc is considerably more extended than is commonly observed for such galaxies (Okamoto et al. 2005). Interestingly, the satellites of the main galaxy in this model provide a good match to the properties of the brightest Milky Way satellites (Libeskind et al. 2007).

Okamoto et al. (2005) presented a third simulation in their paper, the “density-burst” model, which led also to a bulge-dominated object. We do not discuss our analysis of this object in this paper because this galaxy lost most of its baryons in strong galactic winds and is therefore not particularly suitable for studying the evolution of the angular momentum of the baryonic component. Nevertheless, we have checked that the results for this object are qualitatively similar to those of the “bulge-dominated” galaxy.

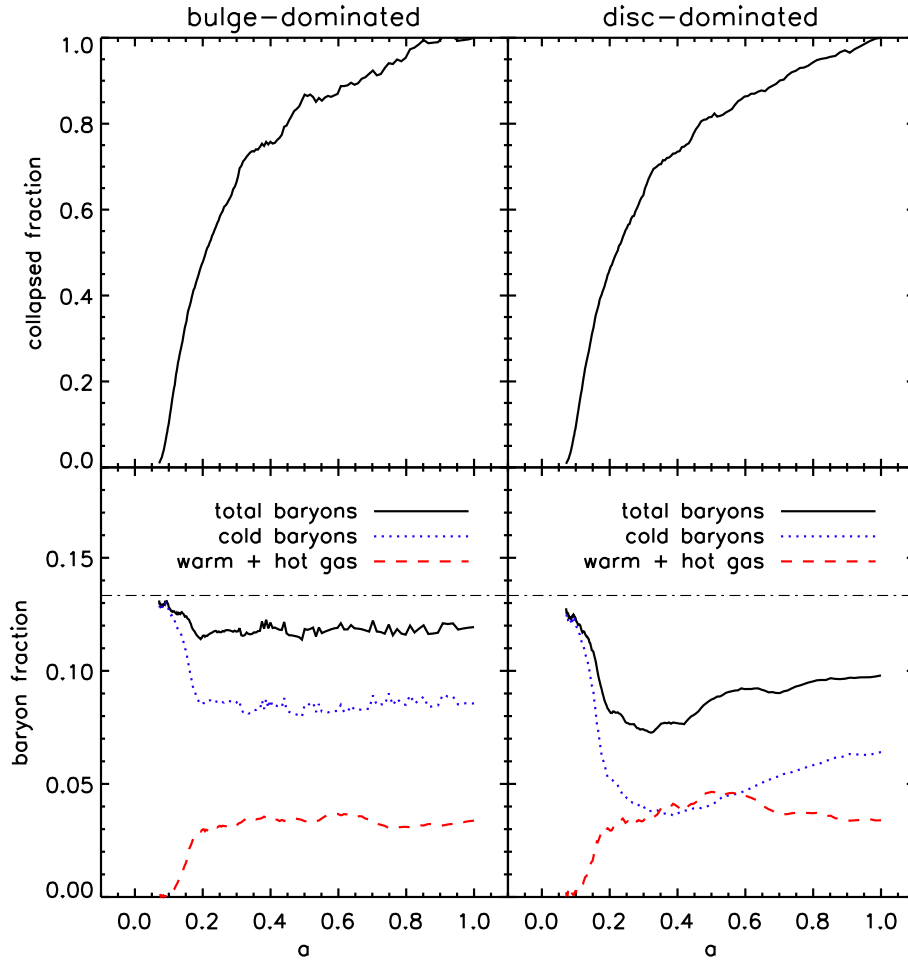


Figure 2. Upper panels: the fraction of the final dark halo mass that is contained in progenitor halos with particle number, $N_{\text{DM}} \geq 10$, at redshift z for the bulge-dominated (left) and the disc-dominated (right) galaxies. Lower panels: baryon fractions in the progenitor halos. The thick solid lines give the total mass fraction of baryons in progenitor halos with $N_{\text{DM}} \geq 10$. The dotted line shows the contribution to this fraction from cold baryons defined to be stars and dense gas with $\rho_g \geq 7 \times 10^{-27} \text{ gr cm}^{-3}$; the dashed line shows the contribution of all other baryons to which we refer as warm/hot gas. The thin line marks the cosmic baryon fraction, Ω_b/Ω_0 . The left panel corresponds to the bulge-dominated galaxy and the right panel to the disc-dominated galaxy.

In our analysis of angular momentum evolution, we distinguish three (Lagrangian) components for each galaxy at $z = 0$. The centre of the system is taken to be the density peak of the stellar distribution. The first component is the dark matter halo which we define as the dark matter mass contained within the virial radius, r_v . We take r_v to be the radius within which the mean density is 100 times the critical value (Eke, Cole, & Frenk 1996). For both galaxies, the halo mass is $\sim 10^{12} h^{-1} M_\odot$ and the virial radius is $\sim 210 h^{-1} \text{ kpc}$. The second component we consider is the *inner Lagrangian halo* which we define as the 10% most bound dark matter particles at redshift $z = 0$. The third component is the “galaxy” which we define as the stars and dense gas ($\rho \geq 7 \times 10^{-27} \text{ g cm}^{-3}$) contained within $0.1 r_v$. In the next section, we will follow the evolution of these three components.

Fig. 1 shows edge-on and face-on views of the surface density of the two galaxies. The bulge-dominated galaxy (left) has a centrally concentrated spheroidal bulge, a small disc and an extended, nearly spherical stellar halo. The disc-dominated galaxy (right) has a small central bulge, an extended disc and a spheroidal stellar halo.

In Fig. 2 we highlight relevant aspects of the global evolution of the Lagrangian region associated with the final dark matter halo. We identify the progenitors of the final halo by applying, at each

redshift, the friends-of-friends grouping algorithm of Davis et al. (1985) to the dark matter particles that end up in the halo at $z = 0$. We employ a linking length, $l_{\text{link}} = b(z)\langle l \rangle$, where $\langle l \rangle$ is the mean dark matter interparticle separation and the linking parameter, $b(z)$, is scaled from the canonical value of 0.2 for an Einstein-de-Sitter universe according to

$$b(z) = 0.2 \left(\frac{\Delta_v(z)}{178} \right)^{-\frac{1}{3}},$$

where $\Delta_v(z)$ is the virial overdensity (relative to the mean) at each redshift. As expected, the evolution of the dark matter component is very similar for the two simulations. The halo builds up rapidly at first and, by $z = 4$, half of the final halo mass is already in place in progenitors of more than 10 particles each. Large mergers are manifest as rapid increases in mass, such as that visible at $z \sim 1.4$.

The evolution of the baryons in the collapsed regions is very different in the two simulations. Initially, all the baryons are assumed to be cold but, as the halo progenitors collapse, their associated baryons are shock-heated and begin to cool radiatively. In the bulge-dominated case, the baryon fraction decreases slightly at first but it soon settles into a quasi-steady state, with a cold fraction (stars plus dense gas with $\rho_g \geq 7 \times 10^{-27} \text{ gr cm}^{-3}$) that is

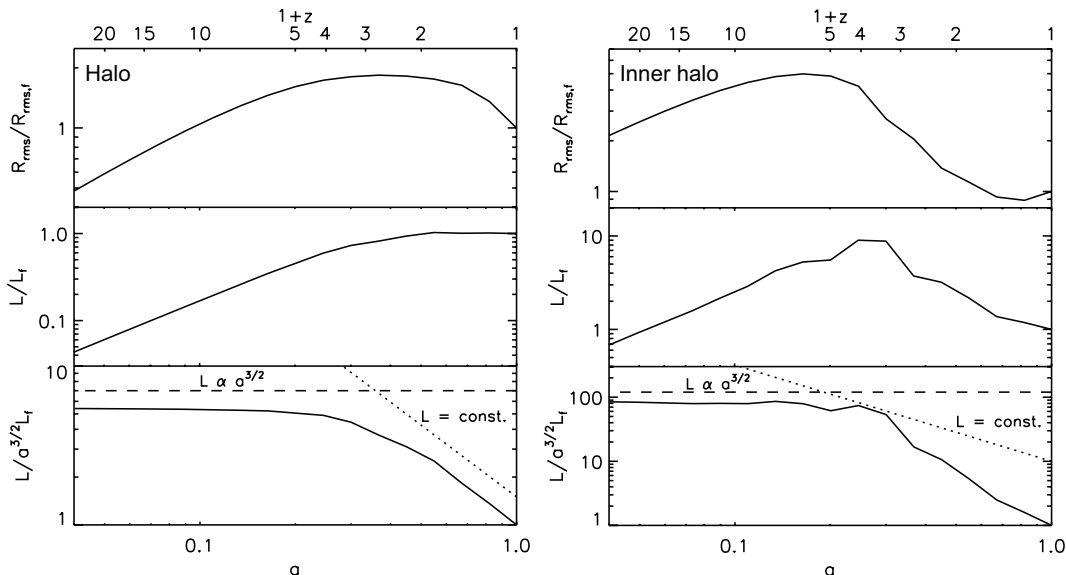


Figure 3. Left: the evolution of the *rms* radius (top panel) and the specific angular momentum (middle and bottom panels) of the dark matter particles that lie within r_v at $z = 0$. In the bottom panel the dashed line indicates $L \propto a^{3/2}$ and the dotted line $L = \text{const.}$ Right: as the left but for the particles that make the inner dark matter halo as defined in Section 2. All physical quantities are normalised to their values at the present day.

approximately 2.5 times larger than the warm/hot fraction (the remaining baryons). The total baryon fraction in the collapsed regions is in excellent agreement with the mean value of $\sim 90\%$ of the cosmic mean found in non-radiative gas simulations of a Λ CDM universe by Crain et al. (2007). By contrast, in the disc-dominated case, strong winds eject almost half of the baryons from the progenitor halos by $z \sim 4$. Some of these, however, are recaptured after $z \sim 1.5$ and the baryon fraction recovers to about 75% of the cosmic mean by the end. The warm/hot phase behaves similarly to the bulge-dominated case, but the cold component is much lower, particularly during the crucial period between $z = 4$ and 1 when much of the merger activity is taking place. The cold baryon fraction increases slightly towards the end, reaching ~ 0.5 of the universal value at the end. In what follows, we shall show how these differences in the history of the baryon content influence the final morphology of the galaxies in a profound way.

3 RESULTS

We now calculate the evolution of the physical (i.e. not the comoving) angular momentum of the particles that make up each of the three components defined in Section 2 at the present day: the total halo, the inner halo and the galaxy. We identify the same particles at each output time in the simulation, find the position and velocity of their centre of mass and compute the physical angular momentum of each system, \mathbf{L}_T , as

$$\mathbf{L}_T = \sum_i \mathbf{l}_i = \sum_i m_i (\mathbf{r}_i \times \mathbf{v}_i), \quad (1)$$

where \mathbf{r}_i and \mathbf{v}_i denote, respectively, the position and velocity of particle i relative to the centre of mass of the system. The total specific angular momentum, \mathbf{L} , is given by $\mathbf{L} = \mathbf{L}_T/M_T$, where M_T is the total mass of the system.

3.1 Dark matter component

First, we focus in the dark matter component. The evolution of the baryons has only a minor effect on the evolution of the halo and so the results are very similar for the bulge- and disc-dominated galaxies as already seen in Fig. 2. We show results only for the latter case.

The top-left panel of Fig. 3 shows the evolution of the physical *rms* radius of the dark matter halo as a function of the scale factor, normalised to the present day *rms* radius. The evolution closely follows the spherical collapse model: the system expands, reaches a maximum radius at $1+z \sim 3$ and begins to collapse at $1+z \sim 2$ to form a virialized system of size about half the radius at maximum expansion. The middle-left panel shows the evolution of the magnitude of the specific angular momentum, $L = |\mathbf{L}|$, of all the dark matter particles that lie within r_v at $z = 0$ as a function of a , once again normalised to the present day value. During the rapidly expanding phase, ($1+z > 4$), the system gains angular momentum in proportion to $a^{3/2}$, as first calculated from tidal torque theory by White (1984). During the collapsing phase, ($1+z < 2$), the magnitude of the angular momentum remains nearly constant. To show the dependence on the scale factor more clearly, in the bottom-left panel of the figure we scale the specific angular momentum by $a^{3/2}$. This plot clearly shows the two distinct evolutionary phases, indicated by the dashed ($L \propto a^{3/2}$) and dotted ($L = \text{const.}$) lines. Our results agree well with previous analyzes of N-body simulations (e.g. White 1984; Catelan & Theuns 1996).

The right panels of Figure 3 show the same quantities as the left panels but now for the particles that make up the inner dark matter halo (i.e. the 10% most bound mass) at $z = 0$. Since this subsystem has a higher overdensity than the halo as a whole, it reaches maximum expansion earlier and begins to collapse at $1+z \sim 5$. The inner halo shrinks more rapidly than the halo as a whole and ends up with a radius that is only about 1/5 of the size at maximum expansion. At $1+z \sim 5$, the particles that will end up in the inner halo are not contained in a single object, but in several subclumps which subsequently merge. This is illustrated in Fig. 4

which shows the spatial distribution of the inner halo particles at $1 + z \simeq 4$ and 3.3. Many of the fragments merge between these two epochs and it is these mergers that determine the evolution of the *rms* size of the system during this period.

The middle and bottom panels of Fig. 3 show that the evolution of the specific angular momentum of the inner halo is very different from that of the halo as a whole. Initially, during the expansion phase, the system gains angular momentum in much the same way as the halo as a whole, roughly following the $L \propto a^{3/2}$ scaling. However, after maximum expansion, ($1 + z < 4$), the inner halo rapidly loses most of its angular momentum. This behaviour is due to the intense merging activity illustrated in Fig. 4. As fragments are drawn towards the centre by dynamical friction, the asymmetric distribution of dark matter produced by gravitational tides exerts a torque which transfers the orbital angular momentum of the fragments to the outer halo. Each merger event is accompanied by a decline in the angular momentum and in this way 90% of the angular momentum is drained from the inner halo. During this phase, the angular momentum of this system declines roughly as a^{-3} . This behaviour was first noted in the early cold dark matter simulations of Frenk et al. (1985). The redistribution of angular momentum during virialization has been studied in detail by D’Onghia & Navarro (2007).

3.2 Bulge-dominated galaxy

We now perform the same analysis on the baryonic component of the bulge-dominated galaxy illustrated in the left panels of Fig. 1. The total stellar mass of this system is $6.75 \times 10^{10} h^{-1} M_{\odot}$ and the total gas mass is $7.5 \times 10^9 h^{-1} M_{\odot}$.

The evolution of the *rms* radius of this galaxy, plotted in the upper-left panel of Fig. 5, is remarkably similar to that of the inner dark matter halo. The system expands until $1 + z \sim 5$ and then collapses. The evolution of the magnitude of the specific angular momentum (lower-left panel) is also very similar to that of the inner dark matter halo. During the expanding phase, the system gains angular momentum in proportion to $a^{3/2}$, as expected from linear theory. After $1 + z \simeq 4$, the system rapidly loses its angular momentum, just as the inner dark matter halo did, transferring it to the outer halo. The decline in the specific angular momentum of the galaxy during the collapsing phase is less abrupt than for the inner halo, scaling roughly a $L \propto a^{-1}$.

The similarity in the behaviour of the bulge-dominated galaxy and the inner halo arises because even before the collapse phase, the cold baryonic material is distributed in a similar way to the mass of the inner halo, as may be seen in Fig. 2. Radiative cooling of gas is very efficient in dense subclumps at early times and, in this simulation, much of the gas cools and turns into stars inside the fragments that will later merge to make the inner halo. Very little gas is left over for later accretion and, as shown in Fig. 2, the cold gas fraction hardly changes between $z = 4$ and the present. Just as in the dark matter only case, the fragments, now containing a mixture of dark matter and cold baryons (stars and dense gas), merge together transferring their orbital angular momentum to the outer halo. With most of the final cold baryons already in place within the fragments at early times, the end result of the collapse and merger phase is a bulge-dominated object.

3.3 Disc-dominated galaxy

We now analyse the disc-dominated galaxy illustrated in the right-hand panels of Fig. 1. This galaxy has $4.17 \times 10^{10} h^{-1} M_{\odot}$ in stars

and $1.53 \times 10^{10} h^{-1} M_{\odot}$ in cold dense gas. The results are shown in the right hand panels of Fig. 5.

The top-right panel of Fig. 5 shows that the baryonic material that will end up in the galaxy expands until $1 + z \simeq 4$ and then begins to collapse. This happens slightly later than for the bulge-dominated galaxy. The lower-right panel shows that, as for all other objects and components, the evolution of the angular momentum during the expanding phase follows linear theory closely, with $L \propto a^{3/2}$. However, unlike the bulge-dominated galaxy, the angular momentum of the system remains nearly constant during the collapsing phase ($1 + z < 3$), indicating that the accreting gas conserves its angular momentum. This behaviour is reminiscent of that of the halo as a whole, illustrated in Fig. 3. Indeed, the lower-right panel of Fig. 5 is very similar to the bottom-left panel of Fig. 3.

The correspondence between the evolution of the angular momentum of the baryonic material of the disc-dominated galaxy and of the material that makes up the halo follows from the similarity of their spatial distributions at the time of maximum expansion. As discussed in Section 2, mergers of subclumps in this simulation induce large-scale shocks in the gas which result in an increased star formation efficiency. This, in turn, produces strong feedback which is further promoted by the assumed top-heavy starburst IMF, keeping the gas out of the merging fragments. Since the merger rate is higher at high redshift, this strong feedback suppresses the early collapse of gas into small proto-galaxies. The process is apparent in Fig. 2: the wind-driven ejection of gas at $z \sim 4$ drastically reduces the cold gas fraction in progenitor halos which remains much smaller than in the bulge dominated galaxy. Thus, most of the baryons that will make up the final galaxy become decoupled from the sub-clumps early on and accumulate in a hot gas reservoir in the main halo. This hot gas has similar specific angular momentum than the halo and, as it loses its pressure support through radiative cooling, it accretes onto the galaxy conserving its angular momentum. The key to the formation of disc galaxies is hence the suppression of the early collapse of baryons into merging fragments, as anticipated by many authors (Navarro & Steinmetz 2000; Okamoto et al. 2005; Sommer-Larsen & Dolgov 2001; Thacker & Couchman 2001; Weil, Eke, & Efstathiou 1998).

Finally, in Fig. 6 we show the evolution of the unnormalised specific angular momentum of the whole halo (solid line) and of the baryonic components of both galaxies, the bulge-dominated (dashed line) and the disc-dominated (dotted line) objects. This figure indicates that it is not only the shape of the time dependence of the angular momentum that is similar between the halo and the baryons of the disc-dominated galaxy, but, remarkably, also the value of the specific angular momentum of the two components. Thus, our simulation provides strong support for the classical theory of disc formation whereby tidally torqued gas is accreted into the centre of the halo conserving its angular momentum (Fall & Efstathiou 1980; Mo et al. 1998). This is the assumption made in semi-analytic models of galaxy formation (e.g. Cole et al. 2000). By contrast, the bulge-dominated galaxy ends up with only about 25% of the specific angular momentum of its halo.

4 DISCUSSION AND CONCLUSIONS

The inability to obtain realistic discs by the present day in simulations from cold dark matter initial conditions has been ascribed to various possible causes: (i) a lack of numerical resolution (Kaufmann et al. 2007; Governato et al. 2004, 2007), (ii) an artificial transfer of angular momentum from a cold disc to

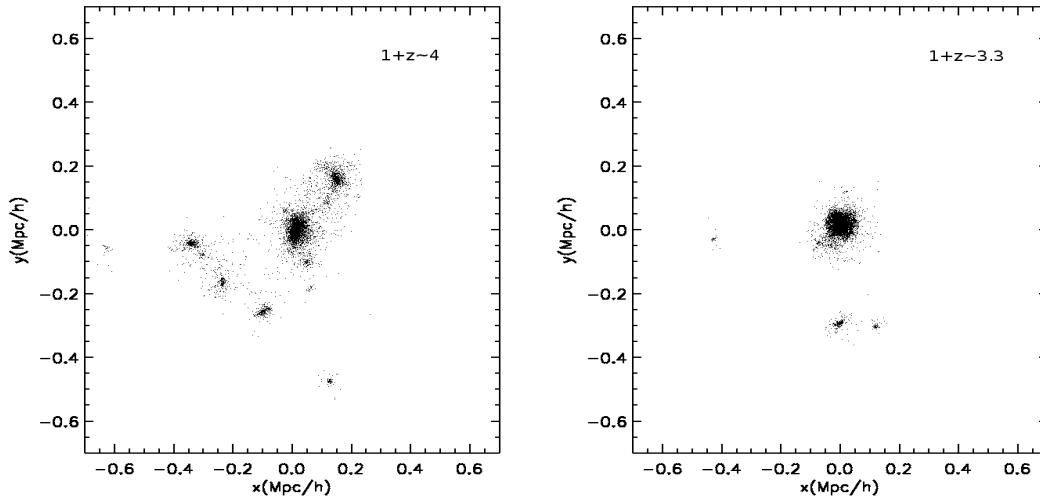


Figure 4. Projected positions of the dark matter particles which will eventually end up in the inner halo at $z = 0$. The left panel shows the distribution at $1 + z \sim 4$ and the right panel at $1 + z \sim 3.3$.

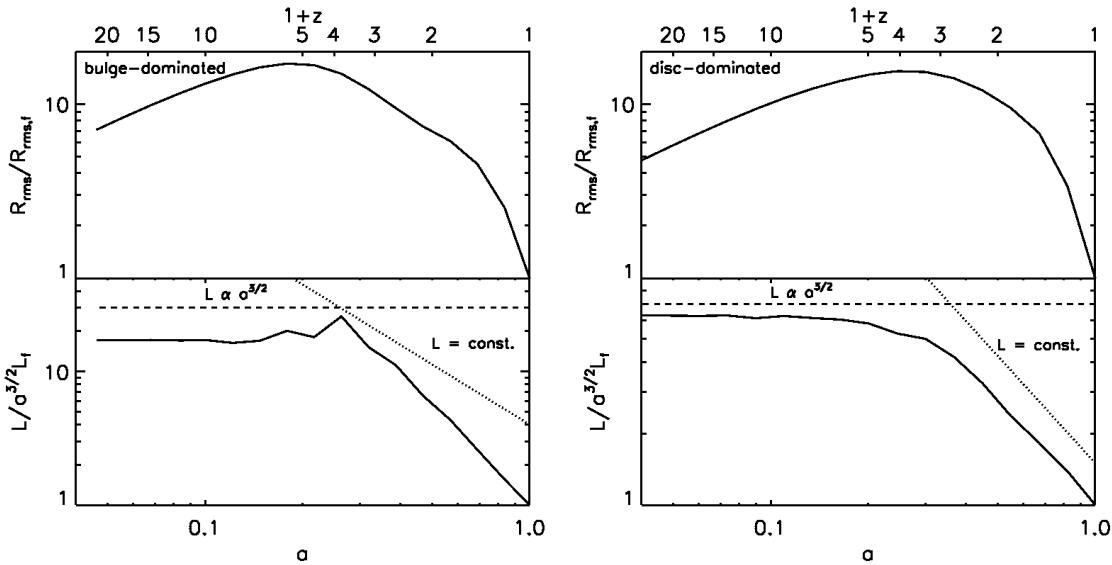


Figure 5. Evolution of the *rms* radius (upper panel) and specific angular momentum (lower panel) with scale factor for the baryonic component. The left panels correspond to the bulge-dominated galaxy and the right panels to the disc-dominated galaxy. All physical quantities are normalized to their value at the present day.

a hot surrounding atmosphere (Okamoto et al. 2003), (iii) instabilities in a heavy disc which, by causing fragments to form, end up transporting angular momentum inwards (Robertson et al. 2004), and (iv) the transfer of angular from merging substructures to the outer halo (Navarro & Benz 1991; Navarro & White 1994; Navarro, Frenk, & White 1995). The first three of these four considerations are unimportant in our simulations. Okamoto et al. (2003) carried out a convergence study which suggests that, so long as the cold and hot gas phases are dynamically decoupled, resolution effects are not important in calculations the size of those we analyse here. Such decoupling also suppresses process (ii). The adoption of an effective multiphase equation-of-state stabilizes a disc against gravitational instability thus alleviating (iii). Process (iv) is inevitable and is the dominant form of angular momentum transport (at least for the dark matter) in our simulations.

The series of N-body/SPH simulations of galaxy formation in a CDM universe carried out by Okamoto et al. (2005) led to the conclusion that galaxies with very different morphologies can form in the same dark matter halo depending on the details of the assumed star formation and feedback prescriptions. In this paper, we have investigated the evolution of the specific angular momentum as a possible explanation for why relatively small differences in the assumed baryonic processes can result in such different outcomes. We have analyzed the bulge-dominated and the disc-dominated galaxies simulated (from identical initial conditions) by Okamoto et al. (2005). We trace back all the dark matter particles that end up within the virial radius of the halo (r_v), as well as those that end up in the central parts of the halo by virtue of being in the top 10 percentile of the binding energy distribution. We also

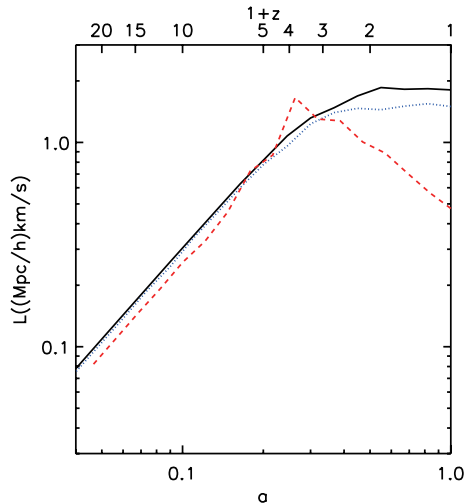


Figure 6. Specific angular momentum of the dark matter component (solid line) and of the baryonic component of the bulge-dominated galaxy (dashed line) and of the disc-dominated galaxy (dotted line).

trace back the baryonic particles that end up as a galaxy, i.e. as cold baryons (star particles and dense gas) within 10% of r_v at $z = 0$.

The angular momentum of the dark matter halo evolves almost identically in the two simulations. The specific angular momentum of the halo as a whole grows initially as predicted by tidal torque theory in the linear regime, in proportion to $a^{3/2}$ (White 1984; Catelan & Theuns 1996). This phase lasts until maximum expansion is reached. Thereafter, the angular momentum of the dark matter remains constant, as the system collapses to a virialized configuration. By contrast, the evolution of the most bound 10% of the dark matter is strikingly different. In the linear phase this material behaves just as the halo as a whole but, after maximum expansion, its specific angular momentum rapidly declines to $\sim 10\%$ of its maximum value. The decline occurs in episodes associated with the mergers that build up the central halo. Most of the angular momentum of these fragments is invested in their orbits and is transferred to the outer halo by tidal forces as the fragments sink by dynamical friction.

The baryonic component evolves very differently in the two simulations. In essence, in the disc-dominated galaxy, the specific angular momentum of the baryons tracks that of the halo as a whole, while in the bulge-dominated galaxy, it tracks the evolution of the central halo material. The reason for the difference can be traced back to the different strengths of feedback in the two galaxies at early times. In the bulge-dominated galaxy, feedback is weak and most of the baryons rapidly cool and condense into stars within sub-galactic fragments. As these halo fragments merge and give up their angular momentum to the outer halo, so do the baryon clumps within them. The result is a slowly-rotating central bulge. A small amount of residual gas rains in later on forming a small disc. In the disc-dominated galaxy, by contrast, feedback is strong at early times, the gas is reheated before it can make a substantial mass of stars and, instead, accumulates in an extended hot reservoir which acquires a specific angular momentum similar to that of the dark halo. By the time this gas is able to cool, much of the merger activity has subsided and so the gas is able to dissipate and collapse into an centrifugally supported disc configuration conserving its angular momentum. Not only does the angular momentum of the baryonic material track the evolution of the angular momentum of the halo, but the actual values of the specific angular momentum of both

components are very similar throughout the entire history of the galaxy. By contrast, the specific angular momentum of the bulge-dominated galaxy is only about 25% of the halo value.

Our results confirm that the key to the formation of disc galaxies in the cold dark matter cosmology is the suppression of the early collapse of baryons into small, dense halos. By contrasting the different evolutionary histories of the angular momentum in bulge- and disc-dominated galaxies, our analysis explicitly reveals how regulating the rate at which gas is supplied determines the final morphology of the galaxy. A disc galaxy results when, as seen in Fig. 2, a large fraction of the baryon content of the halo is ejected by winds at early times. The ejected baryons (some of which are recaptured later) are thus decoupled from the subhalos that are destined to merge and join a hot gas reservoir which is tidally torqued in the same way as the host halo and thus acquires the same net specific angular momentum. Our results provide strong support for the classical theory of disc formation by Fall & Efstathiou (1980) and Mo et al. (1998) in which tidal torques impart the same specific angular momentum to the dark matter and the gas and angular momentum is conserved during disc formation.

ACKNOWLEDGMENTS

This work was carried out during a research visit of JZ to the ICC at Durham supported by the EU's ALFA programme through the Latin American European Network for Astrophysics and Cosmology. JZ acknowledges support from CONACyT and DGEP-UNAM scholarships. We thank Simon White for insightful comments. TO and CSF acknowledge support from PPARC. CSF acknowledges receipt of the Royal Society Wolfson Research Merit Award. The simulations were carried out at the Cosmology Machine at the ICC.

REFERENCES

- Abadi M. G., Navarro J. F., Steinmetz M., Eke V. R., 2003, *ApJ*, 591, 499
- Baugh, C. M., Lacey, C. G., Frenk, C. S., Granato, G. L., Silva, L., Bressan, A., Benson, A. J., & Cole, S. 2005, *MNRAS*, 356, 1191
- Catelan P., Theuns T., 1996, *MNRAS*, 282, 436
- Cole, S., Lacey, C. G., Baugh, C. M., & Frenk, C. S. 2000, *MNRAS*, 319, 168
- Crain R. A., Eke V. R., Frenk C. S., Jenkins A., McCarthy I. G., Navarro J. F., Pearce F. R., 2007, *MNRAS*, 377, 41
- Davis M., Efstathiou G., Frenk C. S., White S. D. M., 1985, *ApJ*, 292, 371
- D'Onghia E., Burkert A., Murante G., Khochfar S., 2006, *MNRAS*, 372, 1525
- D'Onghia E., Navarro J. F., 2007, *MNRAS*, 380, L58
- Eke V. R., Cole, S. M., Frenk C. S., 1996, *MNRAS*, 282, 263
- Fall S. M., Efstathiou G., 1980, *MNRAS*, 193, 189
- Frenk, C. S., White, S. D. M., Efstathiou, G., & Davis, M. 1985, *Nature*, 317, 595
- Firmani C., Avila-Reese V., 2000, *MNRAS*, 315, 457
- Governato F., et al., 2004, *ApJ*, 607, 688
- Governato F., Willman B., Mayer L., Brooks A., Stinson G., Valenzuela O., Wadsley J., Quinn T., 2007, *MNRAS*, 374, 1479
- Kaufmann T., Mayer L., Wadsley J., Stadel J., Moore B., 2007, *MNRAS*, 375, 53
- Kennicutt R. C., Jr., 1998, *ApJ*, 498, 541

- Libeskind N. I., Cole S., Frenk C. S., Okamoto T., Jenkins A., 2007, MNRAS, 374, 16
- Mo, H. J., Mao, S., & White, S. D. M. 1998, MNRAS, 295, 319
- Nagashima M., Lacey C. G., Baugh C. M., Frenk C. S., Cole S., 2005a, MNRAS, 358, 1247
- Nagashima M., Lacey C. G., Okamoto T., Baugh C. M., Frenk C. S., Cole S., 2005b, MNRAS, 363, L31
- Navarro J. F., Benz W., 1991, ApJ, 380, 320
- Navarro J. F., Frenk C. S., White S. D. M., 1995, MNRAS, 275, 56
- Navarro J. F., White S. D. M., 1994, MNRAS, 267, 401
- Navarro J. F., Steinmetz M., 2000, ApJ, 538, 477
- Okamoto T., Eke V. R., Frenk C. S., Jenkins A., 2005, MNRAS, 363, 1299
- Okamoto T., Jenkins A., Eke V. R., Quilis V., Frenk C. S., 2003, MNRAS, 345, 429
- Robertson B., Yoshida N., Springel V., Hernquist L., 2004, ApJ, 606, 32
- Sommer-Larsen J., Dolgov A., 2001, ApJ, 551, 608
- Sommer-Larsen J., Götz M., Portinari L., 2003, ApJ, 596, 47
- Springel, V. 2005, MNRAS, 364, 1105
- Steinmetz M., Navarro J. F., 2002, NewA, 7, 155
- Thacker R. J., Couchman H. M. P., 2001, ApJ, 555, L17
- Weil M. L., Eke V. R., Efstathiou G., 1998, MNRAS, 300, 773
- White S. D. M., 1984, ApJ, 286, 38

This paper has been typeset from a $\text{\TeX}/\text{\LaTeX}$ file prepared by the author.